



Biosynthesis of ZnO NPs Based Resin Nanocomposites: A Sustainable Oral Health Care Solution

SHRAVANI RAMESH WADEKAR^{1*}, MANISH SHAMRAO HATE¹
and RAMESH CHAUGHULE²

¹*Head of the Chemistry Department, Ramnarain Ruia Autonomous College, L.N. Road, Matunga (East), Mumbai-400019, India.

²Ex. Tata Institute of Fundamental Research, Mumbai, India, Adjunct Professor, Ramnarain Ruia Autonomous College, Matunga (East), Mumbai-400019, India.

*Corresponding author E-mail: shravaniwadekar996@gmail.com

<http://dx.doi.org/10.13005/ojc/420137>

(Received: May 31, 2025; Accepted: August 23, 2025)

ABSTRACT

Dental caries is a highly prevalent chronic disease globally, emphasizing the need for sustainable and biocompatible materials in restorative dentistry. This study presents the green synthesis of zinc oxide nanoparticles (ZnO NPs) using *Cassia fistula* leaf extract and their incorporation as nanofillers in resin nanocomposites comprising UDMA, GMA, APTES, and CQ. This formulation serves as a cost-effective substitute for Bis-GMA based products. The formation of ZnO NPs was confirmed using UV-Vis spectroscopy, FTIR, FESEM, HRTEM, XRD, and DLS techniques. Resin nanocomposites with varying compositions of ZnO NPs were synthesized and evaluated for mechanical properties including tensile strength, flexural strength, and compressive strain, and compared to TiO₂ NPs based composites. The optimal formulation with 0.15 g ZnO NPs showed a tensile strength of 1415.53 gf, flexural strength of 16.26 gf, and compressive strain of 71.84% at 0.10 g. Results indicate that ZnO NPs with UDMA, GMA, and APTES offer a sustainable, efficient, and economical alternative to conventional dental materials. Further investigations include cytotoxicity evaluation via MTT assay on fibroblast cell lines (triplicate experimental run), *in vivo* testing, antibacterial and antifungal studies against common oral pathogens, and assessment of synergistic effects with other nanoparticles to enhance efficacy.

Keywords: ZnO NPs, GMA, resin nanocomposites, tensile strength, flexural strength, compression strength.

INTRODUCTION

Dental caries remains one of the most common oral health problems worldwide, affecting individuals across all age groups. According to the World Health Organization, more than 3.5 billion (around 45%) people globally experience toothache

or related complications, making it a pressing public health concern¹. The human oral cavity harbours complex microbial communities that often develop resistance to conventional antimicrobial therapies. If left untreated, dental caries can progress from enamel to dentin, leading to inflammation, infection, necrosis, and ultimately, tooth loss². Furthermore, poor oral



health has been linked to systemic conditions such as cardiovascular disease, diabetes, chronic headaches, auditory complications, and adverse pregnancy outcomes. These associations highlight the urgent need for restorative materials that are not only cost-effective but also capable of preventing infection and promoting long-term oral health³.

Historically, dental materials such as amalgam, cements, and conventional resin-based composites have been employed for restorative procedures⁴. However, these materials present several drawbacks, including inadequate adhesion, marginal leakage, biofilm accumulation, and biocompatibility concerns. Notably, amalgam fillings, which have been used for over a century, have been largely phased out due to their mercury content, which has been associated with neurological and renal toxicity⁵. Additionally, amalgam surfaces tend to promote bacterial colonization, leading to secondary degradation and compromised restoration integrity.

In response to these limitations, nanotechnology has emerged as a transformative solution in dentistry. The incorporation of metal and metal oxide nanoparticles into resin-based composites has shown considerable promise in improving antibacterial performance, mechanical strength, and aesthetic properties⁶. Among the various nanoparticles explored, zinc oxide nanoparticles (ZnO NPs) stand out due to their excellent antibacterial, antifungal, and physicochemical properties. ZnO NPs are notably efficient in disrupting bacterial cell membranes, diminishing biofilm formation, avoiding secondary cavities, exhibiting superior adhesive properties, and maintaining non-toxicity while being ecologically benign.⁷

Crucially, the biosynthesis of ZnO NPs using plant-based extracts offers a green and sustainable alternative to traditional chemical and physical synthesis methods^{8,9}. In this study, we utilized the aqueous extract of *Cassia fistula* leaves to synthesize ZnO NPs through an eco-friendly approach that eliminates the need for toxic reagents and high-energy processes as previously reported¹⁰. These biosynthesized ZnO NPs were then integrated into a resin nanocomposite matrix composed of glycidyl methacrylate (GMA), urethane dimethacrylate (UDMA), and 3-

(aminopropyl) triethoxysilane (APTES), along with the photo-initiator camphorquinone (CQ), to develop a novel dental restorative material. The resulting ZnO NP-based resin nanocomposite exhibits enhanced antibacterial efficacy, superior mechanical stability, and improved adhesion that makes it a viable, sustainable solution for oral healthcare^{11,12}. By combining biocompatibility with eco-conscious synthesis and advanced functional performance, this material represents a promising step toward comprehensive, cost-effective dental care solutions that meet both clinical and environmental goals.

MATERIALS AND METHODOLOGY

All chemicals used in our study were of analytical reagent (A.R.) grade with a reported purity of 100%. UDMA, APTES, CQ, and GMA were obtained from Sigma-Aldrich, Mumbai, India. Polyvinyl alcohol (PVA), acetone, glycerol, distilled water, titanium dioxide nanoparticles (TiO₂ NPs), and commercial zinc oxide powder (ZnO powder) were procured from SRL, Mumbai, India. A commercially available dental composite (Dentsply Spectrum Composite Syringe Restorative Kit; Shade: A2; Batch No.: 2003000436) manufactured by Dentsply Sirona were used as a control.

Cylindrical and disc-shaped Teflon molds (diameter: 6–10 mm; thickness: 1–2 mm; depth: 2 mm) were used for sample preparation. Photopolymerization was conducted utilizing a light-curing apparatus (Model: Woodpecker Mini S, Woodpecker, China) with a 3W high-power blue LED (wavelength range: 420–480 nm; light intensity: 1000–1200 mW/cm²; weight: 150 g).

Synthesis of ZnO NPs

ZnO NPs were synthesized by a previously documented green synthesis process, in which the plant extract served as both the reducing and stabilizing agent, as formerly reported earlier¹⁰. The resulting nanoparticles were characterized through various hyphenated analytical techniques including ultraviolet-visible (UV-Vis) spectroscopy, Fourier transform infrared spectroscopy (FTIR), powder X-ray diffraction (PXRD), field emission scanning electron microscopy (FESEM), high-resolution transmission electron microscopy (HRTEM), and energy dispersive X-ray analysis (EDAX) as established in earlier studies¹⁰.

Preparation of ZnO NPs-Based Resin Nanocomposites

ZnO NPs, prepared using the aforementioned method¹⁰, were used to prepare the resin nanocomposites. Initially, 0.05 g of ZnO NPs were dispersed in 5 mL of APTES in an Erlenmeyer flask. The mixture was stirred using a magnetic stirrer (Remi, 150 W, dimensions: 200×225×185mm, speed range: 15–1500rpm, stirring capacity: up to 800 mL) at 30–40°C for 20–30 min at 500rpm until complete dispersion and solubilization of the ZnO NPs was achieved. Additional APTES was added accordingly if the dispersion appeared dry. In a separate beaker, 0.4 mL of UDMA and 0.6 mL of GMA were mixed without heating using a magnetic stirrer for 20–30 min at 500rpm. This UDMA-GMA mixture was then added to the ZnO NPs-APTES solution and stirred at 50–80°C until a homogeneous, slightly semisolid consistency was obtained and thereafter 0.01 g of CQ was added and stirred vigorously to activate the solution. Subsequently, 0.2 mL–0.5 mL of glycerol was added and stirred without heating to yield a viscous solution.

Separately, 0.1 g of PVA was dissolved in 10 mL of distilled water and stirred at 60°C for 30 min, followed by cooling to obtain a uniform solution. A Petri dish was placed on a magnetic stirrer maintained at 60–70°C, into which the semisolid ZnO NPs-APTES-UDMA-GMA-CQ mixture was introduced. A small amount of the prepared PVA solution (1% w/v) was added, and the entire mixture was blended thoroughly using a spatula to obtain a cohesive semisolid suspension. The final nanocomposite suspension was cast into disc-shaped PTFE-Teflon moulds (2mm depth, 2mm thickness, 10mm diameter). The moulds were air-dried and subsequently photo-cured using a light-curing device positioned 2 cm above the samples. After curing, the specimens were removed from the moulds using a syringe needle. Additionally, resin nanocomposite formulations containing 0.10 g and 0.15 g of ZnO NPs were prepared following the same procedure. These samples were subjected to mechanical characterization, including tensile, flexural, and compressive strength analysis. A schematic representation of the fabrication process is illustrated in Figure 1.

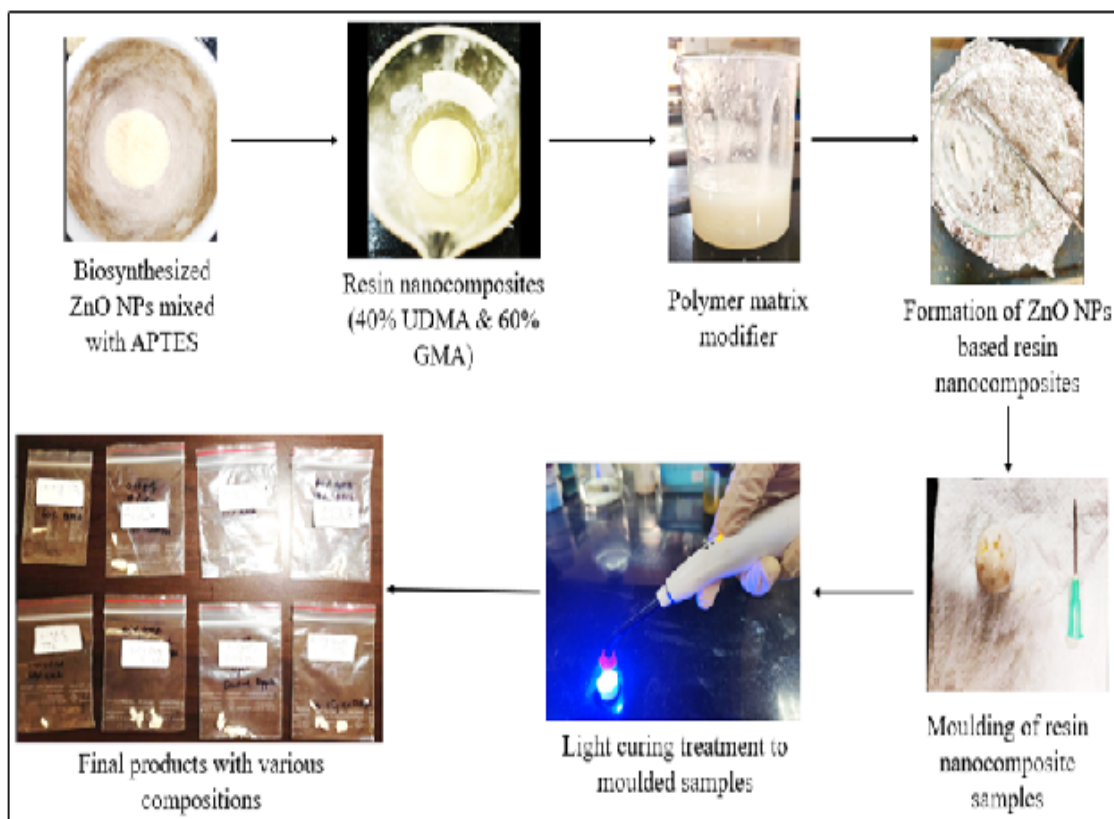


Fig. 1. Schematic representation for the formation of resin nanocomposites using biologically synthesized ZnO NPs

RESULTS

Characterization of ZnO NPs Using Various Analytical Techniques

The synthesized ZnO NP exhibited unique structural and morphological attributes, validated through hyphenated analytical techniques as reported earlier¹⁰.

Tensile Strength Analysis of synthesized resin nanocomposites

Tensile strength analysis was conducted on the resin nanocomposites, incorporated with varying concentrations of ZnO NPs and TiO₂ NPs, as summarized in Table 1. ZnO NPs based resin

nanocomposites (Samples A–F) present the tensile strength results containing ZnO NPs and TiO₂ NPs at concentrations ranging from 0.05 g to 0.15 g. For ZnO NPs (Table 1, Samples A–C), a moderate tensile strength was observed with 0.05 g. However, increasing the concentration to 0.10 g resulted in the lowest tensile strength across the samples. A marked improvement was noted at 0.15 g, where the maximum tensile strength reached 1415.53 gf (gram force). In contrast, TiO₂ NPs (Table 1, Samples D–F) exhibited a different trend. At 0.05 g, the tensile strength was moderate, increasing significantly to a peak value of 1789.0 gf at 0.10 g. However, further increasing the concentration to 0.15 g led to a sharp decline in tensile strength, dropping to 228.09 gf.

Table 1: Tensile strength of ZnO NPs and TiO₂ NPs based resin nanocomposites with varying concentration

Sample number	Specifications of resin nanocomposites	Sample composition	Concentration	Tensile strength (gf)
A	All resin nanocomposites prepared using 0.4mL UDMA+0.6mL GMA	ZnO NPs	0.05 g	463.731
B			0.10g	313.901
C			0.15g	1415.5306
D		TiO ₂ NPs	0.05 g	1693.81
E			0.10g	1789.0
F			0.15g	228.09

Flexural strength analysis of synthesized resin nanocomposites

The flexural strength for ZnO NPs based resin nanocomposite (Table 2, Samples A-C) increases with increasing concentration for 0.05

g to 0.15 g from 10.00 gf to 16.26 gf whereas, the opposite trend is observed with TiO₂ NPs based resin nanocomposite (Table 2, Samples D-F), decreasing with increasing concentration for 0.05 g to 0.15 g from 25.57 gf to 11.14 gf.

Table 2: Flexural strength analysis of ZnO NPs and TiO₂ NPs based resin nanocomposites with varying concentration

Sample number	Specification resin nanocomposite	Sample composition	Concentration	Flexural strength (gf)
A	All resin nanocomposites prepared using 0.4 mL UDMA + 0.6 mL GMA	ZnO NPs	0.05 g	10.00
B			0.10 g	13.38
C			0.15 g	16.26
D		TiO ₂ NPs	0.05 g	25.57
E			0.10 g	20.87
F			0.15 g	11.14

Compression strength analysis of synthesized resin nanocomposites

(i). **ZnO NPs based resin nanocomposite samples (Table 3, Samples A-C):** Demonstrated a highest peak compression percentage of 71.84% for 0.10 g, succeeded by 71.75% for 0.05 g and 71.49% for 0.15 g, respectively.

(ii). **TiO₂ NPs based resin nanocomposite samples (Table 3, Samples D-F):** A contrary tendency is noted for TiO₂ NPs

resin nanocomposites. The maximum compression percentage is 71.83% for 0.15 g, succeeded by 71.58% for 0.10 g and 71.50% for 0.05 g.

(iii). **ZnO NPs and TiO₂ NPs based resin nanocomposites (Table 3, Sample G,H):** Represents samples with 0.1 g and 0.15 g each of ZnO NPs and TiO₂ NPs, respectively, resulting in two distinct concentration samples. The highest percentage of compression, 71.67%, is noted in resin nanocomposite samples containing 0.15 g

- each of ZnO NPs and TiO₂ NPs, followed closely by samples with 0.10 g each of the same components at 71.58%.
- (iv). **Spectrum samples:** 0.01g each of ZnO NPs, TiO₂ NPs, and commercial ZnO powder were combined individually with 0.1 g each of a commercial spectrum sample and subjected to a compression test as detailed in (Table 3, Samples I-K). The highest percentage of compression recorded was 28.05% for ZnO powder, 100.04% for ZnO NPs, and 19.95% for TiO₂ NPs.

Table 3: Compression testing of ZnO NPs and TiO₂ NPs based resin nanocomposites, including hybrid and commercial spectral samples

Sample number	Sample composition	Specification of resin nanocomposite	Concentrations	Maximum compression load (Newton)	Maximum compression strain (%)
A	ZnO NPs	All resin	0.05 g	13.75	71.75
B		nanocomposites	0.10 g	13.87	71.84
C		prepared using	0.15 g	06.81	71.49
D	TiO ₂ NPs	0.4mL UDMA	0.05 g	37.70	71.50
E		+0.6mL GMA	0.10 g	18.58	71.58
F			0.15 g	09.21	71.83
G	ZnO NPs+TiO ₂ NPs		0.1 g+0.1 g respectively	05.80	71.58
H	ZnO NPs+TiO ₂ NPs		0.15 g+0.15 g respectively	14.88	71.67
I	TiO ₂ NPs	-	0.01 g TiO ₂ NPs in 0.1 g of spectrum (commercial)	1684.00	19.95
J	ZnO NPs	-	0.01g ZnO NPs in 0.1 g of spectrum (commercial)	1532.76	100.04
K	ZnO Powder	-	0.01 g ZnO Powder in 0.1 g of spectrum (commercial)	33.18	28.05

DISCUSSION

Tensile strength analysis

Both ZnO NPs and TiO₂ NPs have superior mechanical characteristics at appropriate concentrations^{13,14}. Effective dispersion of nanoparticles enhances the interfacial interaction between the nanoparticles and the metacrylate of nanocomposites, hence improving tensile strength^{15,16}. Nonetheless, the agglomeration of nanoparticles leads to diminished mechanical strength owing to decreased interfacial contact¹⁷⁻¹⁹. ZnO NPs demonstrate superior tensile strength at elevated concentrations (0.15 g) in contrast to TiO₂ NPs, which display comparable findings at a reduced concentration of 0.05 g (Table 1, Sample A-F). The differences arise from the elevated surface energy of TiO₂ NPs by interaction with air and moisture, owing to the presence of hydroxyl (-OH) groups on their surface²⁰. TiO₂ NPs efficiently absorb water molecules from the environment, which then dissociate on the surface to generate terminal and bridging hydroxyl groups, thereby enhancing their surface reactivity²¹. These groups establish strong interfacial interactions with the resin matrix, facilitating effective stress transfer and enhancing resistance to failure under

external loads²²⁻²³. As the concentration of TiO₂ NPs rises to 0.15 g, agglomeration may occur, interrupting the light-curing process²⁴⁻²⁶. Moreover, TiO₂ NP possesses a high refractive index (2.6-2.9), resulting in enhanced light scattering during the curing process. This dispersion may lead to partial polymerization, resulting in porosity (defects/voids) inside the resin matrix. Conversely, ZnO NPs exhibit superior performance at elevated concentrations (0.15 g) owing to their enhanced dispersion and strong interfacial interaction with the resin matrix, facilitating more efficient stress distribution²⁷⁻²⁸. Moreover, ZnO NPs possess a lower refractive index compared to TiO₂ NPs, resulting in less light scattering. This guarantees enhanced polymerization efficiency and inhibits the emergence of flaws such as opacity or air voids.

Flexural strength analysis

ZnO NPs have superior flexural strength at a higher concentration (0.15 g) relative to TiO₂ NPs, primarily attributable to enhanced dispersion within the resin matrix and the establishment of strong interfacial bonding. This improved dispersion, facilitates efficient stress distribution, leading to enhanced flexural strength²⁹. The reduced refractive index of ZnO NPs enhances the polymerization

process, resulting in a more stable final composite. Conversely, TiO₂ NPs have superior flexural strength at a lower concentration (0.05 g), but this strength diminishes as the concentration rises to 0.15 g. At elevated concentrations, the aggregation of TiO₂ NPs may occur, compromising the resin matrix and adversely impacting the polymerization process. The incomplete polymerization, along with the eventual formation of air gaps or defects, results in decreased flexural strength and overall mechanical performance³⁰.

Compression analysis

ZnO NPs at 0.05 g yield a higher percentage compression as compared to TiO₂ NPs, mostly due to better dispersion of nanoparticles, surface activity and strong interfacial bonds between resin composite (Table 3, Sample A). As concentration increases to 0.15 g, the compression activity decreases mostly due to agglomeration of nanoparticles (Table 3, Sample B, C). The reverse trend is observed with TiO₂ NPs (Table 3, Samples D, F). When binary composites ZnO NPs are combined with TiO₂ NP with 0.1 g each, it a lower value for percentage compression than with 0.15 g each. Hence, with increase in concentration the difference observed is 9.0% (Table 3, Sample G, H). This could be due to multiple factors; the co-addition may lead to differences in surface energy and particle size which may lead to weakening of the structural integrity of the composite and hence reducing matrix reinforcement³¹. In summary, the expected synergistic effect may not be observed with the combination of ZnO NPs and TiO₂ NPs as observed using nanoparticles, alone.

However, when combined with spectrum, it shows a higher percentage compression for ZnO NPs (100.04%) and the lowest for TiO₂ NPs (19.95%), attributed to the difference in resin-nanoparticles interaction³². ZnO NPs may agglomerate with the spectrum resin, leading to weaker reinforcement and more deformation with the highest percentage compression, hence showing higher flexibility (Table 3, Sample J). In contrast, TiO₂ NPs show better dispersion, providing structural support and the highest compression load with low percentage compression and get deformed easily under stress (Table 3, Sample I). Moreover, when combined with ZnO powder commercially, it shows a moderate percentage compression along with the lowest

compression load than the other two, implying its least ability for structural integration due to its large size and surface area³³⁻³⁵. This could be because commercial ZnO may not bond effectively with the commercial spectrum as effectively as with TiO₂ NPs, leading to the higher deformation, though the overall strength is moderate³⁶⁻³⁸. Hence, out of three, TiO₂ NPs and ZnO NPs outperformed well than commercial ZnO in restorative dental composites, with TiO₂ NPs bearing maximum load and ZnO NPs with maximum flexibility.

Future Scope

Samples with more than 99% compression strain suggest their potential use in applications where flexibility is important. However, this property can be optimized by eliminating nanoparticle agglomeration and adjusting the concentration and morphological characteristics. Therefore, future studies should focus on modifying the material to enhance its suitability for restorative applications. Additionally, biocompatibility studies of ZnO NPs-based resin nanocomposites are recommended through cytotoxicity evaluation (MTT assay) and antibacterial assays to determine their minimum inhibitory concentrations (MIC), along with comparisons to TiO₂ NPs to ensure safe use³⁹⁻⁴¹. These materials should also be made eco-friendly to ensure long-term stability without degradation. Recently, 3D printing has shown promising applications in restorative dentistry; hence, the prepared resin nanocomposites could be explored for 3D printing compatibility to improve both clinical and material outcomes⁴². Furthermore, these materials can be investigated for use in various dental fields, including endodontics, orthodontics, periodontics, implantology, cosmetic dentistry, and preventive dentistry, due to their enhanced properties and biocompatibility⁴³. It is worth investigating the impact of nanoparticle shape (e.g., rods, sheets, spheres) on resin reinforcement behaviour. It is necessary to scale up nanocomposite synthesis using green and cost-effective methods for broader commercial applications in dental, biomedical, and structural materials. The impact of integrating antibacterial agents on the depth of cure, degree of conversion, microleakage, and bond strength to enamel and dentin, alongside their compatibility with different adhesive systems, necessitates comprehensive *in vitro* examination; furthermore, *in situ* studies are recommended to

assess the influence of human saliva and the oral environment on the antibacterial, mechanical, and physical properties of resin nanocomposites⁴⁴.

CONCLUSION

This study shows that nanoparticles concentration, refractive index, adhesive bonding, particle size, and surface energy greatly affect the mechanical properties of resin-based nanocomposites. At lower concentrations, TiO₂ NPs exhibited higher tensile and flexural strength, possibly due to good dispersion in the resin matrix. At higher concentrations, particle aggregation and surface contact led to agglomeration, reducing mechanical performance. TiO₂ NPs also demonstrated remarkable stiffness and structural stability, with the lowest compression percentage and highest compressive load among the evaluated materials.

ZnO NPs showed better tensile and flexural strength at moderate concentrations, likely due to improved nanoparticle dispersion and resin-matrix interaction. However, at slightly lower concentrations, the percentage compression was highest, indicating potential agglomeration and structural weakness. Compared to the commercial spectrum resin, ZnO NP-incorporated samples demonstrated greater compression

strain with moderate compressive force, suggesting enhanced flexibility, elasticity, and better compatibility with the resin, likely aided by surface modification. In contrast, the commercial ZnO powder, composed mostly of larger particles, provided minimal mechanical reinforcement due to poor dispersion, trace impurities, and limited interfacial interaction with the resin. At higher concentrations, both ZnO and TiO₂ NPs showed increased compression strain, possibly due to particle interference and disrupted nanoparticle–resin bonding, emphasizing the necessity for meticulous tuning of nanoparticle incorporation in dental nanocomposite formulations.

ACKNOWLEDGEMENT

The Authors would like to express sincere gratitude to the Dr. P.S. Ramanathan laboratory at Ramnarain Ruia Autonomous College, ICT (Institute of Chemical Technology) in Matunga, IIT (Indian Institute of Technology) Mumbai, and ICON labs in Navi Mumbai for characterization and data analysis. Special thanks to Dr. HeereshShetty from Nair Hospital for his guidance and support.

Conflict of interest

The authors hereby declare that there is no conflict of interest among themselves.

REFERENCES

- World Health Organization, **2022**. [Website]
- Femiano, F.; Femiano, R.; Femiano, L.; Jamilian, A.; Rullo, R.; Perillo, L., *Eur. J. Paediatr. Dent.*, **2016**, *17*, 243.
- Comeau, P.; Burgess, J.; Malekafzali, N.; Leite, M. L.; Lee, A.; Manso, A., *Materials*, **2022**, *15*, 5075.
- Ferracane, J. L., *J. Funct. Biomater.*, **2024**, *15*, 173.
- Raorane, D. V.; Chaughule, R. S.; Pednekar, S. R.; Lokur, A., *Saudi Dent. J.*, **2019**, *31*, 194.
- Naguib, G.; Maghrabi, A. A.; Mira, A. I.; Mously, H. A.; Hajjaj, M.; Hamed, M. T., *BMC Oral Health.*, **2023**, *23*, 1.
- Bourgi, R.; Doumandji, Z.; Cuevas-Suárez, C. E.; Ammar, T. B.; Laporte, C.; Kharouf, N.; Haikel, Y., *Coatings*, **2025**, *15*, 33.
- J., N.; K., E.; R. S., *Resour. Chem. Mater.*, **2024**, *3*, 294.
- Bouttier-Figueroa, D. C.; Cortez-Valadez, M.; Flores-Acosta, M.; Robles-Zepeda, R. E., *Bio Nano Science.*, **2024**, *14*, 3385.
- Wadekar, S. R.; Hate, M. S.; Chaughule, R., *Orient. J. Chem.*, **2025**, *41*.
- Ok, I.; Aykac, A., *Chem. Pap.*, **2023**, *77*, 6959.
- Matei, A.; Cernica, I.; Cadar, O.; Roman, C.; Schiopu, V., *Int. J. Mater. Form.*, **2008**, *1*, 767.
- Tiwari, A. K.; Jha, S.; Singh, A. K.; Mishra, S. K.; Pathak, A. K.; Ojha, R. P.; Yadav, R. S.; Dikshit, A., *Crystals*, **2022**, *12*, 1063.
- Zhang, O. L.; Niu, J. Y.; Yin, I. X.; Yu, O. Y.; Mei, M. L.; Chu, C. H., *Dent. J.*, **2023**, *11*, 59.
- Chaughule, R.; Raorane, D.; Pednekar, S.; Dashaputra, R., *Nanocomposites and Their Use in Dentistry.*, **2018**, 59–79.
- Alfaawaz, Y. F.; Alamri, R.; Almohsen, F.; Shabab, S.; Alhamdan, M. M.; Ahdal, K.

- A.; Farooq, I.; Vohra, F.; Abduljabbar, T., *Scanning*, **2022**, 1–9.
17. Shirkavand, S.; Moslehifard, E., *DOAJ*, **2014**, 8, 197.
18. AlGhamdi, M. A.; Alatiyyah, F. M.; Dawood, Z. H. A.; Alshaikhnasser, F. Y.; Almedarham, R. F.; Alboryh, S. Y.; Elakel, A.; Akhtar, S.; Khan, S. Q.; Gad, M. M., *J. Prosthodont.*, **2024**.
19. Balhaddad, A. A.; Garcia, I. M.; Mokeem, L.; Alsahafi, R.; Collares, F. M.; De Melo, M. a. S., *Bioengineering*, **2021**, 8, 146.
20. Hammer, B.; Wendt, S.; Besenbacher, F., *Top. Catal.*, **2010**, 53, 423.
21. Nayak, R. K.; Mahato, K. K.; Ray, B. C., *Composites Part A Appl. Sci. Manuf.*, **2016**, 90, 736.
22. Azmy, E.; Al-Kholy, M. R. Z.; Fattouh, M.; Kenawi, L. M. M.; Helal, M. A., *Int. J. Biomater.*, **2022**, 1–9, 2022.
23. Naguib, G.; Maghrabi, A. A.; Mira, A. I.; Mously, H. A.; Hajjaj, M.; Hamed, M. T., *BMC Oral Health*, **2023**, 23, 1.
24. Khlifi, K.; Atallah, M. S.; Cherif, I.; Karkouch, I.; Barhoumi, N.; Attia-Essaies, S., *Surfaces Interfaces*, **2023**, 41, 103279.
25. Gad, M. M.; Abualsaud, R.; Al Thobity, A. M.; Baba, N. Z.; Al Harbi, F. A., *J. Prosthodont.*, **2020**, 29, 422.
26. Alhotan, A.; Yates, J.; Zidan, S.; Haider, J.; Silikas, N., *Materials*, **2021**, 14, 2659.
27. Pai, E.; Nayak, A.; Hallikerimath, R. B.; Ruttonji, Z.; Astagi, P.; Pokale, S., *J. Indian Prosthodont. Soc.*, **2023**, 23, 127.
28. Nguyen, T. M. T.; Wang, P.; Hsu, H.; Cheng, F.; Shieh, D.; Wong, T.; Chang, H., *Mater. Sci. Eng. C*, **2018**, 97, 116.
29. Omar, M. H.; Amin, M. H.; Younis, H. A., *Appl. Phys. A*, **2022**, 128, 4.
30. Dias, H. B.; Bernardi, M. I. B.; Bauab, T. M.; Hernandez, A. C.; De Souza Rastelli, A. N., *Dent. Mater.*, **2018**, 35, e36.
31. Raja, T.; Devarajan, Y.; Kailiappan, N., *Discover Applied Sciences*, **2024**, 6, 11.
32. Vikram, S.; Chander, N. G., *Eur. Oral Res.*, **2020**, 31, 35.
33. Ferracane, J. L., *Dent. Mater.*, **2010**, 27, 29.
34. Ahuja, D.; Akhila, M. R.; Singh, A. K.; Batra, P., *J. Int. Oral Health*, **2024**, 16, 439.
35. Kundie, F.; Azhari, C. H.; Muchtar, A.; Ahmad, Z. A., *J. Phys. Sci.*, **2018**, 29, 141.
36. Almoharib, B. K.; Alshammari, O. M.; Alonazi, R. S.; Alshehri, A. A.; Alanazi, M. A.; Alqubaysi, H. A.; Alshammari, A. F.; Alzuhair, N. A.; Alenizi, A. A.; Khormi, F. A.; Alshammari, M. H.; Al-Mutairi, N. H., *Int. J. Health Sci.*, **2023**, 7, 3341.
37. Lizymol, P. P.; Vibha, C.; Deepu, D. R.; Waghmare, S., *ORMO*, **2024**, 48, 211–224.
38. Duraisamy, R., *Int. J. Dent. Oral Sci.*, **2021**, 4380, 4387.
39. Anzabi, R. M.; Divband, B.; Tukmachi, M. S.; Vahedifar, S.; Esmaeilzadeh, M.; Sefidan, F. Y.; Jahanbani, M.; Rafighi, A., *Int. J. Dent.*, **2025**, 1.
40. Jowkar, Z.; Moaddeli, A.; Shafiei, F.; Tadayon, T.; Hamidi, S. A., *Clin. Exp. Dent. Res.*, **2024**, 10, 1.
41. Saini, R.; Vaddamanu, S. K.; Kanji, M. A.; Quadri, S. A.; Hassan, S. a. B.; Anil, S.; Shrivastava, D.; Srivastava, K. C., *BMC Oral Health*, **2024**, 24, 1.
42. Balestra, D.; Lowther, M.; Goracci, C.; Mandurino, M.; Cortili, S.; Paolone, G.; Louca, C.; Vichi, A., *Materials*, **2024**, 17, 1380.
43. Jeong, M.; Radomski, K.; Lopez, D.; Liu, J. T.; Lee, J. D.; Lee, S. J., *Dent. J.*, **2023**, 12, 1.
44. Algarni, A. A., *Cureus*, **2024**.